

Exciton–excitonic molecule Rabi splitting in an inorganic-organic layered semiconductor: Inapplicability of the giant oscillator strength model

Makoto Shimizu*

Frontier Research System, RIKEN, 2-1 Hirosawa, Wako 351-0198, Japan

(Received 13 February 2004; revised manuscript received 25 June 2004; published 31 January 2005)

The resonant Rabi splitting of the exciton–excitonic molecule transition in an inorganic-organic layered semiconductor ($(\text{C}_6\text{H}_5\text{C}_2\text{H}_4\text{NH}_3)_2\text{PbI}_4$), has been investigated by means of the subpicosecond pump-probe spectroscopy. From the observed absorption peak energies as functions of the pump light intensity, the dipole moment of the exciton–excitonic molecule transition per exciton is estimated to be $3.5 \pm 0.4 \text{ e}\text{\AA}$, which is considerably smaller than that estimated from the giant oscillator strength model. This inapplicability of the conventional model is ascribed to the strong polaritonic effect.

DOI: 10.1103/PhysRevB.71.033316

PACS number(s): 78.70.-g, 78.67.-n, 78.47.+p

Excitonic molecules,^{1,2} which are bound states of two excitons, are found in many ionic semiconductors. The strong two-photon resonance for generating the molecules has been well explained to be due to the *giant oscillator strength effect*,^{3,4}

$$\frac{f_m}{f_x} = \frac{\mu_m^2}{\mu_x^2} \approx 2 \frac{[\int g(\mathbf{r})d^3\mathbf{r}]^2}{v_0}, \quad (1)$$

where f_x and f_m represent the oscillator strength *per unit cell* for generating an exciton and the oscillator strength *per exciton* for generating a molecule when excitons are present, respectively. Corresponding transition dipole moments are denoted as μ_x and μ_m , respectively. v_0 and $g(r)$ represent the volume of a unit cell and the wave function of the center-of-mass motion of two constituent excitons, respectively. Namely, a molecule is generated, when a photon is absorbed in the volume of a molecule. The light-exciton interaction has been treated perturbatively after the molecule wave function is determined.

In this decade, the importance of the adequate account of the light-exciton interaction for the molecule has been pointed out theoretically.⁵⁻⁷ In systems where the light-exciton interaction is comparative to the exciton–exciton interaction, these two interactions should be considered simultaneously without the adiabatic approximation. A molecule should be instead understood as a *bipolariton*. Ivanov *et al.* showed that the radiative width, the Lamb shift, and the non-linear susceptibility are precisely given only in the bipolariton model.⁶ So far, the theory has been verified in only several experiments. The above-mentioned quantities and the dispersion curve have been precisely investigated in CuCl ,^{6,8,9} which show quantitative agreements with the bipolariton model. The coherent dynamics in CdS has also been explained with the bipolariton model.¹⁰ However, it has been intriguing whether the oscillator strength of the molecule can be much smaller than that expected with the giant oscillator strength model. In fact, Eq. (1) has been applicable not only to the above-mentioned substances¹¹⁻¹⁵ but also to most of the semiconductors.¹⁶

In our previous work,¹⁷ we derived $\mu_m^2/\mu_{\text{exciton}}^2 \approx 0.6$ for phenomenologically explaining the detuning dependence of

the excitonic optical Stark shift in an inorganic-organic layered semiconductor ($(\text{C}_6\text{H}_5\text{C}_2\text{H}_4\text{NH}_3)_2\text{PbI}_4$, (PhE-PbI₄)). Here, μ_{exciton} ($\neq \mu_x$) represents the exciton transition moment which is *not* normalized by the number of the related unit cells. It is noted that μ_{exciton} is generally not equal to μ_x because of the translational extension of the exciton wave function. A similar result was also derived for explaining the four wave mixing experiment in a similar substance ($(\text{C}_6\text{H}_{13}\text{NH}_3)_2\text{PbI}_4$).¹⁸ In these studies, it was suggested that μ_m relative to μ_{exciton} was small, unlike those in other substances. Nevertheless, it was not possible to test the giant oscillator strength model, because μ_m was not concretely determined, which should be compared with μ_x , but not with μ_{exciton} .

The target substance in this work is PhE-PbI₄, the crystal structure of which was reported in Ref. 19. The cross sectional view of the crystal structure is schematically drawn in Fig. 1. The inorganic and organic layers are perpendicular to the cross section. Low energy excitations, such as excitons, are confined in inorganic layers. Organic layers work as barriers for the confinement. Because of the *dielectric confinement effect*,^{20,21} the exciton Rydberg and the binding energy of the excitonic molecule are 220 meV and 45 meV, respec-

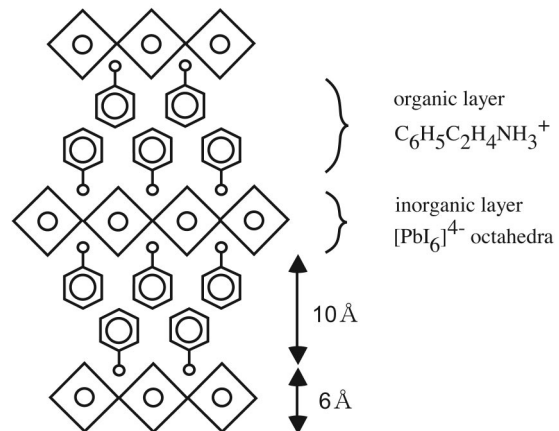


FIG. 1. Schematic cross sectional view of the PhE-PbI₄ crystal. The cross section is perpendicular to layers.

tively. The exciton has a two-dimensional envelope with an in-plane Bohr radius of 14.2 \AA .²¹

In this paper, the author reports the resonant Rabi splitting of the exciton–molecule transition, observed by means of the subpicosecond pump-probe spectroscopy. From the intensity dependence of the splitting, the dipole moment of the exciton–molecule transition per exciton is estimated to be $\mu_m = 3.5 \pm 0.4 e\text{\AA}$. The inapplicability of the giant oscillator strength model is clarified.

PhE-PbI₄ was prepared by the synthetic method.²⁰ The sample for the measurement was a polycrystalline film which was spin-coated on the glass substrate from solution. It is known that the layers of each polycrystalline domain are parallel to the substrate. The sample was placed on the cold finger of the cryostat and was cooled to ca. 10 K.

Photoinduced spectrum change was measured by means of the pump-probe spectroscopy in the transmission geometry. A 1 kHz Ti-sapphire regenerative amplifier was used as the light source. One of the split-off beams was used for generating the pump light with an optical parametric amplifier. The other beam was used for generating the white light continuum as the probe light by the self-phase-modulation in a water cell. The time origin, i.e., the zero delay between pump and probe pulses, was carefully checked with a $\beta\text{-BaB}_2\text{O}_4$ crystal by folding the beam paths in front of the cryostat with a mirror. Since the probe light had a strong chirp, the wavelength dependence of the delay time was numerically corrected for obtaining spectra at particular delay times after the measurement.

In order to obtain the precise value of the transition dipole, special care was taken for estimating the pump intensity. Intensity distributions of pump and probe beams at the sample position were measured with a $\phi = 70 \mu\text{m}$ pinhole whose position was controlled with a micrometer stage. The distributions were estimated to be Gaussian with standard deviations of $\sigma_p = 80 \mu\text{m}$ and $\sigma_t = 89 \mu\text{m}$ for pump and probe beams, respectively, by the deconvolution analysis. Both the autocorrelation trace of the pump pulse and the cross-correlation trace between pump and probe pulses were approximately Gaussian. Accordingly, pump and probe pulses were assumed to have Gaussian time profiles with deviations of $\tau_p = 87.3 \text{ fs}$ and $\tau_t = 58.5 \text{ fs}$, respectively. Based on these parameters, the mean pump intensity experienced by the probe light was estimated as

$$\begin{aligned} \langle I_p \rangle_t &= \frac{\int I_p f(t, \tau_p) f(\mathbf{r}, \sigma_p) I_t f(t, \tau_t) f(\mathbf{r}, \sigma_t) dt d^3\mathbf{r}}{\int I_t f(t, \tau_t) f(\mathbf{r}, \sigma_t) dt d^3\mathbf{r}} \\ &= I_p (2\pi)^{-3/2} (\tau_p^2 + \tau_t^2)^{-1/2} (\sigma_p^2 + \sigma_t^2)^{-1}, \end{aligned} \quad (2)$$

where I and $f(x, \sigma)$ represent the pulse energy and the normalized Gaussian distribution function with the variable of x and the standard deviation of σ , respectively. Subscripts, p and t , denote pump and probe (test) lights, respectively.

The pump photon energy was 2.305 eV , which is below the exciton resonance by $\approx 50 \text{ meV}$. Thus, the pump photon is in close resonance with the transition between the exciton and the molecule, although a slight detuning is concluded

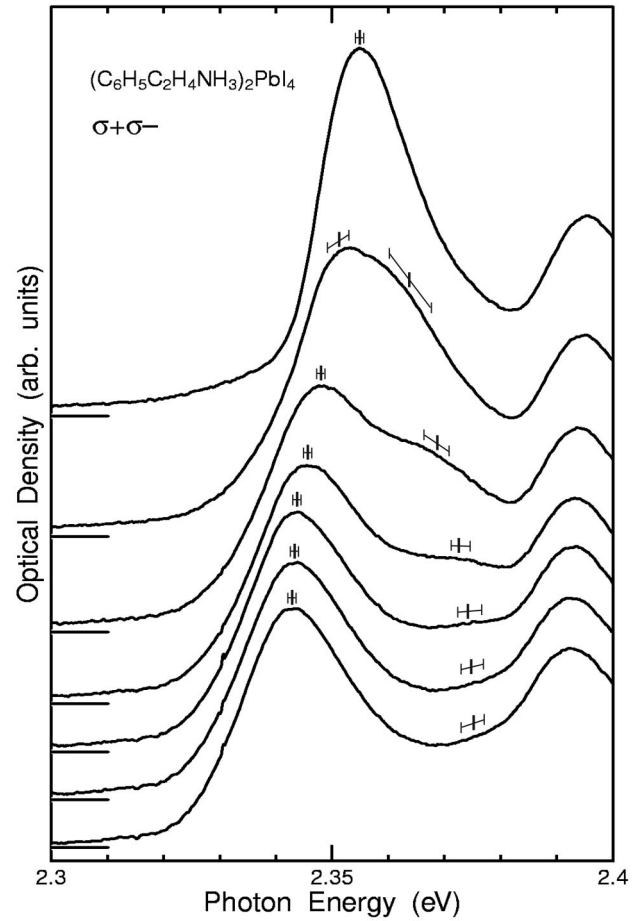


FIG. 2. Pump intensity dependence of the exciton absorption spectrum. Intensities are 0, 0.78, 1.75, 2.73, 3.71, 4.68, and 5.66 GW/cm^2 , from the top to the bottom. Vertical bars show peak energies. Possible errors are suggested with horizontal bars.

from the analysis described below. The pump intensity was controlled with a rotary variable neutral density filter of which transmissivity had been known as a function of the position in order to minimize the error in the measurement of the pump power.

It might be noteworthy that there are two main error sources in estimating μ_m . The one is the quality of the overlap between pump and probe beams on the sample, although the overlap was carefully optimized by means of video telescope. The error is estimated to be $\pm 30\%$ in the pump intensity. The other source is the uncertainty in estimating peak energies in observed spectra. Errors depend on spectra. These errors will be clearly shown in the figures.

Figure 2 shows the intensity dependence of the exciton absorption spectrum. Pump and probe lights were opposite-circularly polarized.²² Pump intensities $\langle I_p \rangle_t$ were 0, 0.78, 1.75, 2.73, 3.71, 4.68, and 5.66 GW/cm^2 , from the top to the bottom. With the zero pump intensity, the peak observed at 2.355 eV is the exciton of our interest. The peak seen at 2.39 eV is ascribed to the exciton of another electronic band, because a unit cell consists of two formula units. It is clearly observed that the main exciton absorption band splits as the pump intensity increases,²³ although the intensity of an upper

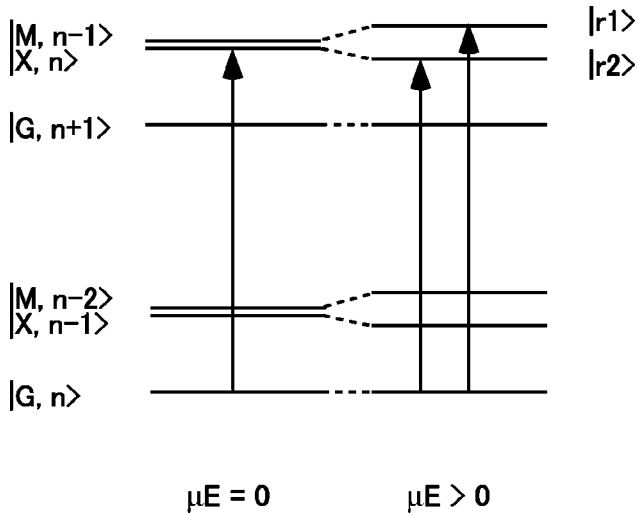


FIG. 3. Schematic diagram for the Rabi splitting. Levels without and with the electron-photon interaction are shown in left- and right-hand sides, respectively. Vertical arrows show transitions observed in the spectra.

band is much lower than that of a lower band. Peak energies were determined manually, because the numerical deconvolution analysis of spectra was not possible due to line shapes. Possible error ranges are estimated as are shown with horizontal bars.

The splitting is explained to be due to the Rabi splitting of the transition between the exciton and the molecule, as is schematically shown in Fig. 3. G , X , and M denote the electronic ground state, the exciton, the excitonic molecule, respectively. Photon numbers are represented as n , $n+1$, etc. Two renormalized states of our interest are marked as $r1$ and $r2$. Considering the close resonance of the pump energy to the exciton-molecule transition, we can neglect any other off-diagonal terms except for the exciton-molecule coupling²⁴ (and this is the reason why μ_m can be reasonably determined, independent of models^{17,18}). On this assumption, the absorption peak energies $\hbar\omega_{\text{abs}}$ are given as²⁵

$$\hbar\omega_{\text{abs}} = \hbar\omega_{|r1\rangle,|r2\rangle} - \hbar\omega_{|G,n\rangle} = \hbar\omega_x - \frac{1}{2}\delta \pm \frac{1}{2}\sqrt{\delta^2 + (\mu_m E)^2}, \quad (3)$$

where $\hbar\omega_x$, $\delta \equiv \hbar\omega_p - \hbar\omega_x + \epsilon_m$, and E denotes the bare exciton energy, the detuning, and the electric field of the pump light. ω_p and ϵ_m denote the pump frequency and the binding energy of the molecule, respectively. For $\mu_m E = 0$, energies of $|X, n\rangle$ and $|M, n-1\rangle$ are only different by a detuning, among which only $|X, n\rangle$ can couple with $|G, n\rangle$ by the probe light. For $|\mu_m E| > 0$, $|X, n\rangle$ and $|M, n-1\rangle$ are mixed to cause larger splitting. Corresponding transitions to the observed peaks are shown with vertical arrows in Fig. 3.

Because the ratio of $|X, n\rangle$ and $|M, n-1\rangle$ components of renormalized wave functions is quite sensitive to the detuning, a slight detuning causes a large difference in the oscillator strengths of the two split bands. This explains the low intensity of the observed upper band. Although the author intended the pump energy to be in the resonance, the exact resonance was hardly achieved. This was partly because the

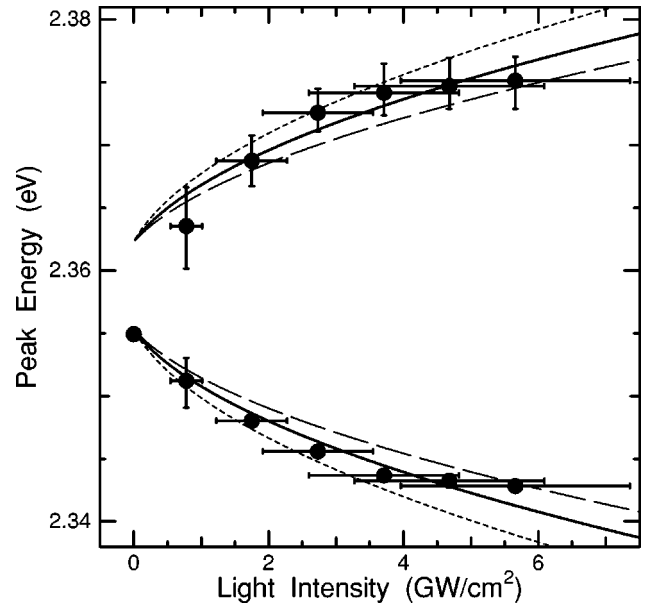


FIG. 4. Peak energies as functions of the pump intensity. Curves are drawn according to Eq. (3). Solid curves show the best fit with $\mu_m = 3.51 e\text{\AA}$. Dashed and dotted curves are drawn with $\mu_m = 3.08$ and $3.92 e\text{\AA}$, respectively.

resonant frequency was not exactly estimated due to the line-widths of the exciton and the excitonic molecule. For the result shown in Fig. 2, a detuning of -7 meV is concluded, according to the analysis given below. When the absolute value of the detuning is even slightly larger, only one shifted band is observed,²³ which is usually called the Stark shift.

It is noted that the splitting is not seen, if pump and probe lights are co-circularly polarized. Instead, the strong blue-shift is observed.¹⁷ This polarization dependence is explained to be due to the following polarization selection rule for the exciton-molecule coupling.²⁶ Only excitons in the spin-singlet combination are allowed for realizing a molecule.

Observed peak energies are plotted as functions of the pump intensity in Fig. 4. The solid curve shows the best fit by Eq. (3) with parameters of $\mu_m = 3.51 e\text{\AA}$, $\delta = -7$ meV, and $\hbar\omega_x = 2.355$ eV. Dashed and dotted curves are drawn with $\mu_m = 3.08$ and $3.92 e\text{\AA}$, respectively, so as to show the largest and smallest possible estimates. The obtained value is close to that ($4.2 e\text{\AA}$) in CuCl.¹³

On the other hand, the exciton dipole moment per unit cell, μ_x , is estimated from the longitudinal-transverse splitting (Δ_{LT}) as $\mu_x = \sqrt{\Delta_{\text{LT}} \epsilon_b} / 4\pi N_0$, where $N_0 = v_0^{-1} = 8.13 \times 10^{20} \text{ cm}^{-3}$ (Ref. 19) and $\epsilon_b = 4.46$ (Ref. 20) represent the number of unit cells per volume and the high frequency dielectric constant. Hong *et al.*²⁰ estimated Δ_{LT} to be 50 meV from the reflectance spectrum in the direction normal to the layers. According to this value, μ_x is estimated to be $1.23 e\text{\AA}$. Therefore, we obtain $f_m/f_x = 2.85^2 = 8.14$ as the experimental value.

The giant oscillator strength effect expressed as Eq. (1) seems not applicable to PhE-PbI₄. Because the wave function of the molecule in PhE-PbI₄ has not been estimated yet in any way, we shall temporarily assume that a molecule has a disklike shape and that its radius is equivalent to the exci-

TABLE I. Comparison between PhE-PbI₄ and CuCl in terms of the exciton Rydberg (ϵ_x), the binding energy of molecules (ϵ_m), the exciton transition moment per unit cell (μ_x), f_m/f_x determined experimentally, and f_m/f_x expected with the giant oscillator strength model [Eq. (1)].

	PhE-PbI ₄	CuCl
ϵ_x	220 meV (Ref. 20)	190 meV (Ref. 27)
ϵ_m	45 meV (Ref. 20)	32 meV (Ref. 11).
μ_x	1.2 eÅ	0.08 eÅ (Ref. 13)
μ_m	3.5 eÅ	4.2 eÅ (Ref. 13)
f_m/f_x	8.1	2500 (Ref. 13), 4000 (Ref. 14)
$2[\int g(\mathbf{r})d^3\mathbf{r}]^2/v_0$	≥ 17	3200 (Ref. 14)

ton Bohr radius ($a_B=14.2$ Å), which should be far smaller than the real radius of the molecule. The volume of a molecule is then $[\int g(\mathbf{r})d^3\mathbf{r}]^2=\pi a_B^2 \times 16.2$ Å³, while the volume of a unit cell is $v_0=6.19 \times 6.13 \times 32.43$ Å³. Accordingly, f_m/f_x is 16.7 from Eq. (1). The experimentally determined ratio is considerably smaller than this value estimated as the smallest limit. If we postulate the twice of a_B as a realistic value for the molecule radius, f_m/f_x is estimated to be even larger, i.e., 66.7. Therefore, the inapplicability of the giant oscillator strength model is concluded.

The role of the polaritonic effect for the molecule in PhE-PbI₄ is made clear, in comparison with facts of CuCl. PhE-PbI₄ and CuCl take similar values in both the exciton Rydberg (ϵ_x) and the molecule binding energy (ϵ_m). Related parameters are summarized in Table I. In CuCl, the giant oscillator strength effect is clearly seen,^{13,14} although the bi-

polariton model might give more precise estimates in other details.⁶ There is a fundamental difference between two substances in μ_x , which determines the ratio of exciton and photon parts of a polariton wave function. In the bipolariton model, the generation of a molecule is achieved by the scattering of two polaritons in the volume of a molecule. Since only the exciton part is responsible for the scattering cross section, the scattering is considered to be far less frequent in PhE-PbI₄. Whereas, in many other substances, the exciton part of the polariton is so large that the bipolariton model and the giant oscillator strength model are indistinguishable in terms of f_m/f_x .

Finally, it is noted that the small f_m/f_x itself in PhE-PbI₄ is not solely due to the polaritonic effect. The two-dimensionality of the exciton makes the volume effect of the molecule less effective. In fact, even with the giant oscillator strength model, f_m/f_x for PhE-PbI₄ is estimated to be much smaller than that for CuCl, as is described above. Polaritons in PhE-PbI₄ have only small opportunity of the scattering for creating molecules, because the interacting range is limited to the same plane of an inorganic layer.

In conclusion, the dipole moment of the excitonic molecule, μ_m , has been determined to be 3.5 ± 0.4 eÅ in an inorganic-organic layered semiconductor, from the resonant Rabi splitting. The oscillator strength ratio of the molecule to the exciton, f_m/f_x , is found to be considerably smaller than that estimated according to the giant oscillator strength model. The inapplicability of the giant oscillator strength model is ascribed to the extremely strong light-exciton interaction.

The author is grateful to Dr. Ryo Shimano and Professor Makoto Kuwata-Gonokami for fruitful suggestions. The work was partly supported by the grant-in-aid for the young scientists (B) (No. 15740189) of MEXT, Japan.

*Electronic address: shimizoo@riken.jp

¹A. Mysyrowicz *et al.*, Phys. Lett. **26A**, 615 (1968).
²H. Souma *et al.*, J. Phys. Soc. Jpn. **29**, 697 (1970).
³E. Hanamura, Solid State Commun. **12**, 951 (1973); J. Phys. Soc. Jpn. **39**, 1516 (1975).
⁴A. A. Golovin and E. I. Rashba, JETP Lett. **17**, 478 (1973).
⁵A. L. Ivanov and H. Haug, Phys. Rev. B **48**, 1490 (1993).
⁶A. L. Ivanov *et al.*, Phys. Rev. B **52**, 11 017 (1995).
⁷A. L. Ivanov *et al.*, Phys. Rep. **296**, 237 (1998).
⁸H. Kawano *et al.*, J. Lumin. **76-77**, 75 (1988).
⁹E. Tokunaga *et al.*, Phys. Rev. B **59**, R7837 (1999).
¹⁰C. Mann *et al.*, Phys. Rev. B **64**, 235206 (2001).
¹¹G. M. Gale and A. Mysyrowicz, Phys. Rev. Lett. **32**, 727 (1974).
¹²N. Nagasawa *et al.*, J. Phys. Soc. Jpn. **39**, 987 (1975).
¹³R. Shimano and M. Kuwata-Gonokami, Phys. Rev. Lett. **72**, 530 (1994).
¹⁴H. Akiyama *et al.*, Phys. Rev. B **42**, 5621 (1990).
¹⁵A. Kuroiwa *et al.*, Solid State Commun. **18**, 1107 (1976).
¹⁶E. Hanamura and H. Haug, Phys. Rep. **33**, 209 (1977); X. Kling-shirn and H. Haug, Phys. Rep. **70**, 315 (1981).
¹⁷M. Shimizu *et al.*, Phys. Rev. B **69**, 155201 (2004).
¹⁸J. Ishi *et al.*, Phys. Rev. B **63**, 073303 (2001).

¹⁹J. Calabrese *et al.*, J. Am. Chem. Soc. **113**, 2328 (1991).
²⁰X. Hong *et al.*, Phys. Rev. B **45**, 6961 (1992); T. Ishihara *et al.*, Surf. Sci. **267**, 323 (1992).
²¹E. A. Muljarov *et al.*, Phys. Rev. B **51**, 14 370 (1995).
²²Circular polarization was realized with achromatic wave plates. Polarization purity was estimated to be better than 99%.
²³The splitting was observable only when the pump photon energy is in very close resonance with the transition energy between the exciton and the molecule. Thus, the observed splitting is clearly distinguished from an artifact due to the imperfect polarization of the probe light.
²⁴Rigorously, the coupling between the ground state and the exciton by the pump light may also influence the observed splitting, as it will slightly raise the energy of $|r2\rangle$. However, this contribution is negligible within our resolution, according to the experimental result that observed absorption energies by $|r1\rangle$ and $|r2\rangle$ are almost symmetric around $\hbar\omega_x - \delta/2$, as seen in Fig. 4.
²⁵P. Mester and M. Sargent III, *Element of Quantum Optics* (Springer, Berlin, 1990).
²⁶M. Combescot, Phys. Rev. B **41**, 3517 (1990).
²⁷A. Goldmann, Phys. Status Solidi B **81**, 9 (1977).